

PACS: 81.07.Gf
UDC: 530.1/539.8

Ultrathin ZnO nanowires fabricated by using low-temperature pulsed laser deposition

A. Shkurmanov

*Peter Grünberg Institute for Semiconductor Nanoelectronics (PGI-9), Research Center Jülich,
52425 Jülich, Germany
(previously: Felix-Bloch-Institute for Solid State Physics, Universität Leipzig,
Linnéstraße 5, 04103 Leipzig, Germany)*

ORCID: 0000-0001-8751-0924

DOI:10.26565/2222-5617-2018-28-04

Recently, numerous devices use ZnO nanowires (NWs) as building blocks, for example, light emitters, pressure and gas sensors, resonators and many others. However, for integrations of the NWs into such devices, a high level of NW diameter control is needed. In this work, an opportunity to adjust the NW diameter by using differently doped by Al or Ga seed layers is presented. Moreover, a change of the doping concentrations allows to optimize the growth temperature. Thus, ultrathin NWs, i.e. with a diameter of $d < 10$ nm can be fabricated by using temperature of $T = 400^\circ\text{C}$. This temperature is far below than those typically used for the fabrication of NWs by pulsed laser deposition.

Keywords: nanowires, ZnO, pulsed laser deposition

Нанодроти з ZnO використовуються в якості ключових елементів для розробки численних пристроїв, таких як світловипромінювачі, сенсори тиску газу, резонатори і багато інших. Для інтеграції нанодротів в такі пристрої потрібна висока точність в регулюванні їх діаметра. Більш того, температура зростання нанодротів грає ключову роль для їх інтеграції. Дані про особливості росту нанодротів при температурах нижче $T = 550^\circ\text{C}$ і інформація про механізми їх зростання дуже обмежені. У цій роботі доведена можливість регулювання діаметра нанодротів за допомогою використання підкладок, легованих Al або Ga. Встановлено, що варіація концентрації домішок в підкладці дозволяє оптимізувати температуру зростання нанодротів. Показано, що можуть бути виготовлені ультратонкі нанодроти з діаметром $d < 10$ nm при температурі $T = 400^\circ\text{C}$. Ця температура значно нижче значення, яке зазвичай використовується для зростання нанодротів методом імпульсно-лазерного осадження.

Ключові слова: нанопроволоки, ZnO, імпульсно-лазерне осадження.

Introduction

ZnO is a transparent conductive oxide which attracts a lot of scientific interest in the last years. This material mostly crystallizes in the hexagonal wurtzite structure by using an ambient pressure and temperature. In the ZnO lattice structure each Zn ion is encircled by a tetrahedral of O ions, and vice-versa which causes a polar symmetry along the hexagonal axis, i.e. ZnO tends to form c-oriented structures with Zn-terminated (0001) or O-terminated (000 $\bar{1}$) polar faces [1]. The polarity is responsible for most of ZnO properties, e.g. piezoelectricity and spontaneous polarization [1, 2]. Additionally, a wide bandgap of about 3.37 eV, optical transparency in the visible spectrum range, large exciton binding energy of about 60 meV at room temperature [3], self-grown properties, radiation hardness, biocompatibility and high melting point of $T = 1950^\circ\text{C}$ make the ZnO favorable semiconductor material for the fabrication of the numerous nanostructures with further integration of them in different applications [1,4].

Fabrication of the cylindrical elongated ZnO nanostructures such as nanowires (NWs) is of a special

interest in this work. The NWs have a high surface-to-volume ratio, can be grown dislocation-free and have many potential applications, e.g. light emitters [5], electromechanical resonators [6], pressure and 3D imaging sensors [7,8]. The desired geometry of the NWs is determined by the applications. For instance, for the pressure sensors, thick NWs with a diameter of $d > 100$ nm are favorable for compression-force application, whereas thin NWs ($d < 100$ nm) are interesting to be used for a bending-force application. Additionally, thin NWs are desired for gas sensors, since sensing is strongly depends on the surface-to-volume ration of the nanostructures. For the ultrathin NWs with a diameter comparable with a Bohr radius, i.e. $d < 10$ nm, quantum confinement effects are expected and these NWs can be used for a fabrication of qubits [9].

Recently, most of the known growth methods use a vapor to solid phase transfer with an epitaxial fabrication of the NWs on the solid substrate. The growth mechanisms can be splitted into two main groups - mechanisms which require presence of a catalyst, or a catalyst-free growth [10]. A catalytic material changes the melting and evaporation points of ZnO, and supports a

chemical reaction. However, the main disadvantage of using a catalyst for the growth process is its diffusion and incorporation into the NW which can lead to a change of the material properties, e.g. conductivity, optical transmission, etc. Obviously, that for a control of chemical purity of the ZnO NWs, which can be required for many of their possible applications, a catalyst-free growth is desired. However, this desired growth mechanism is technically challenged for the most known growth techniques [10,11].

Methods

In order to grow the NWs by a catalyst-free epitaxial growth, a two-steps fabrication process was used. In the first step, a planar Al- or rather Ga-doped ZnO seed layers were fabricated on the a-plane sapphire substrates by using a conventional low-pressure pulsed laser deposition (LP PLD) with a growth temperature of about $T = 720^{\circ}\text{C}$ and oxygen partial pressure of $p = 0.01$ mbar. These seed layers have a doping concentration in a range of $x = 0 - 7$ at% and a thickness of about 200 nm [12]. For the second step, a combination of the sapphire substrate with a seed layer was put into the high-pressure pulsed laser deposition chamber (HP PLD). For more than a decade, the high pressure pulsed laser deposition is using for the NW and other quasi 1-dimensional nanostructure growth [13]. This growth method is technically simple, allows to obtain the NWs by a direct transfer of the depositing ZnO from the vapor to the solid phase without using any catalyst and chemical reaction [10]. Also, a selective growth of the nanostructures is possible by using HP PLD technique [15]. In contrast to the conventional LP PLD method, the high pressure one exploits an internal gas flow which support the transfer of the particles from the target to the substrate, increases a supersaturation of the ZnO particles over the substrate and thus, leads to the growth of the quasi 1- or rather 3-dimensional structures

[10, 11]. The HP PLD growth chamber used for this research is schematically presented in Fig. 1. The body of the chamber is made by quartz and the design of the chamber supports the transfer of the ZnO particles to the substrate.

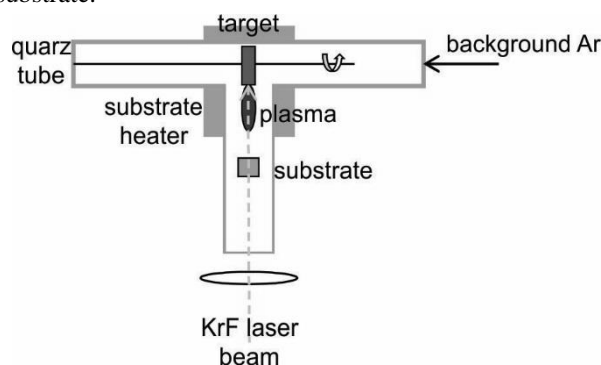


Fig. 1. Scheme of the high-pressure PLD process (top view)

A pulsed high-power excimer laser beam with a wavelength of $\lambda = 248$ nm is focused by a UV lens onto the ZnO target, which is evaporated, excited and ionized. The plasma plume propagates with angle of about 30° towards the substrate's surface. The argon particles are mixed with Zn^+ and O^- ions, reduce their energy and thus the ZnO molecules and clusters can be formed during the transfer to the substrate and be deposited there. After reaching the surface of the substrate, Ar with an excess of the ZnO clusters can be removed in the end of the quartz chamber. Note, that the pressure of the Ar flow is about 150 mbar [13].

However, the most of the reports which use the HP PLD process show the growth of thick NW arrays with typical diameter in a range between 60 and 600 nm [13,15,16,17]. Here, an opportunity to obtain ultrathin NWs by using a different compositions of the underlying seed layers will be shown. Moreover, a choice of the seed layer has a strong impact on the growth temperature

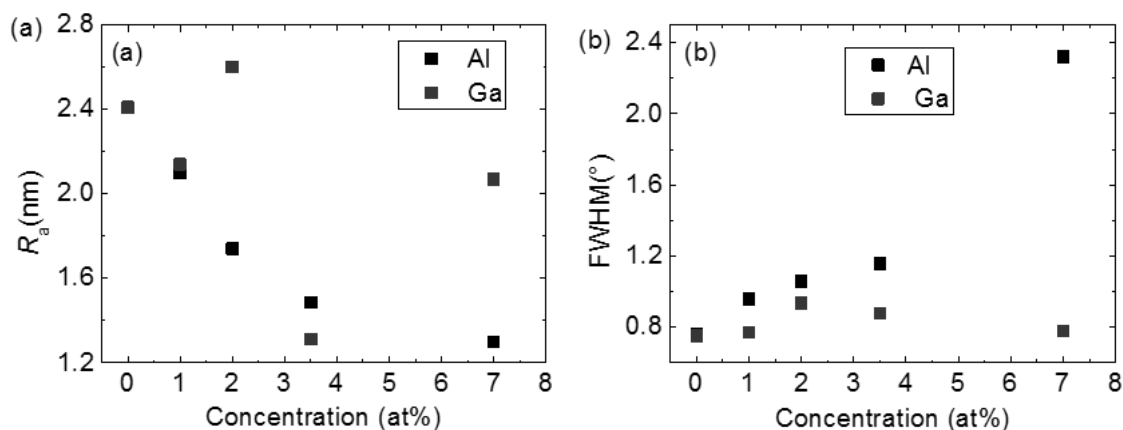


Fig. 2. Surface roughness (a) and the FWHM of rocking curves (b) of the seed layers as a function of the Al or rather Ga concentrations

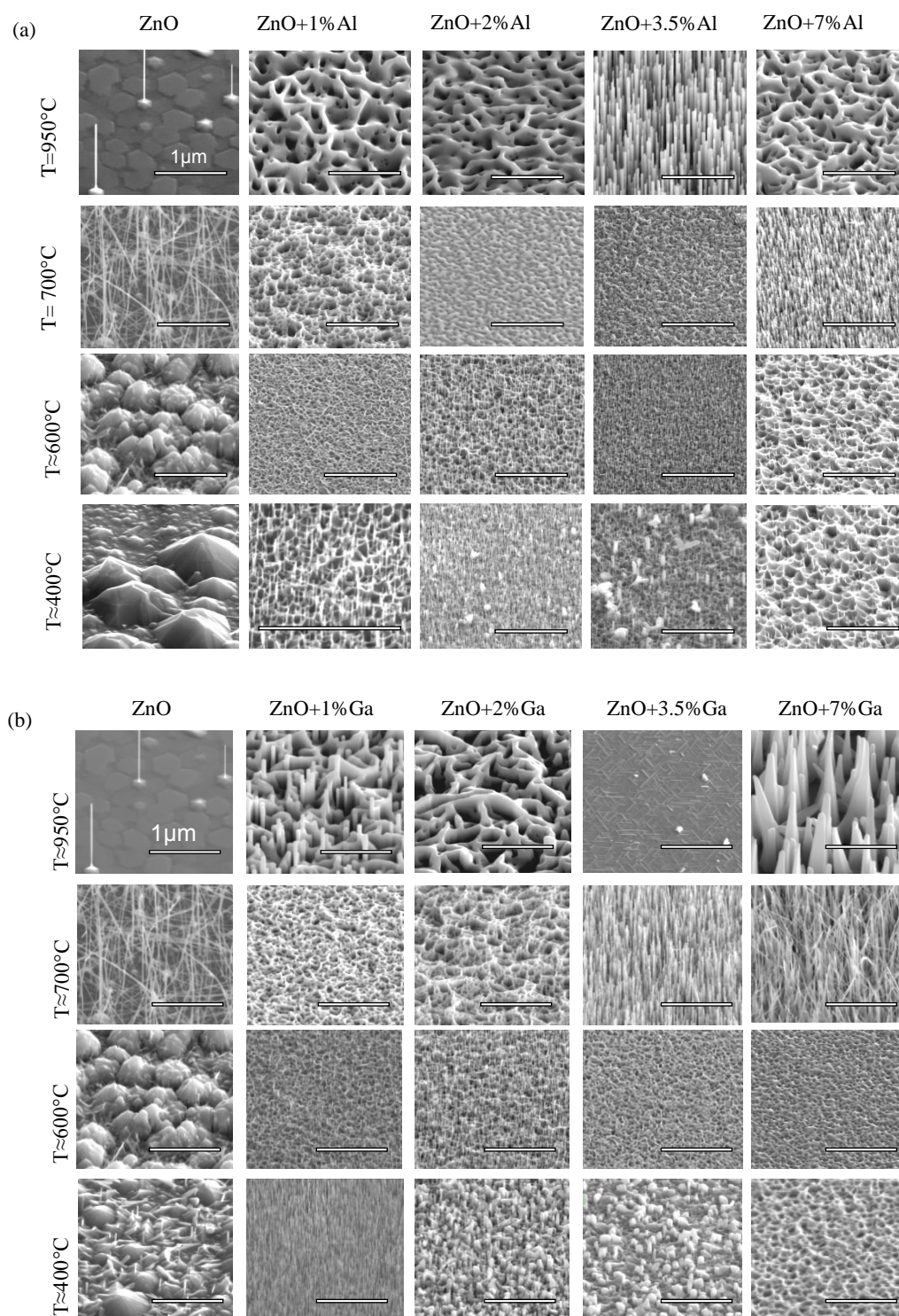


Fig. 3. SEM images of the growth results obtained on the Al-doped (a) or Ga-doped ZnO seed layers (b) by using different temperatures. The scale bar corresponds to 1 μm

which can be strongly reduced from the typical $T = 950^{\circ}\text{C}$ to $T = 400^{\circ}\text{C}$. This relatively low growth temperature can preserve complementary metal-oxide-semiconductor (CMOS) structure [18] and thus, ZnO NWs can be integrated in these technology.

Results

The surface morphology and the crystalline quality of the obtained seed layers were investigated by atomic force

microscopy (AFM) and X-ray diffraction (XRD) measurements, respectively, since the surface can influence the NW's growth [19]. For both types of the seed layers, a quite smooth surface was obtained, as shown in Fig. 2a. However, for the Al-doped ZnO seed layers, a decrease of the average surface roughness from 2.4 to 1.3 nm with increasing Al concentration can be seen. For the Ga-doped seed layers, there is no clear behavior of the average surface roughness as a function of

the doping concentrations and the surface roughness fluctuates typically between 2.0 and 2.6 nm and only for the layer doped with $x = 3.5$ at% of Ga, a reduction of the surface roughness to $R_a = 1.3$ nm can be observed.

The full width half maximum (FWHM) of the rocking curves as a function of the Al and Ga doping concentrations is presented in Fig. 1b. For the undoped ZnO seed layer, FWHM of about 0.8° is observed. For the Al-doped seed layers, an increase of the FWHM up to 2.4° for $x = 7$ at% is seen whereas for the Ga doping, there is no strong dependence on the Ga concentration. In this case, the FWHM was determined to be in the range of 0.8° – 1.0° . The FWHM values are strongly depend on the grain size [20,21] and their tilting, therefore the sizes and tilt of the grains for the Ga-doped seed layers are similar, whereas for the Al-doped layers they increase with increasing of doping concentration.

Scanning electron microscopy (SEM) images of the grown nanostructures are shown in Fig. 3. By using an undoped ZnO seed layer and the high growth temperature of $T = 950^\circ\text{C}$, a low density of vertically oriented NWs is obtained as expected from the previous results [22,23]. These NWs have a diameter of about 70 nm and an aspect ratio of about 25. By reducing the growth temperature down to $T = 700^\circ\text{C}$, diameter of the NWs decreases to 16 nm and aspect ratio increases up to 300. However, in contrast to the NWs prepared by using the highest growth

temperature, these NWs are randomly oriented. For the low temperature growth at $T = 400^\circ\text{C}$, a suppression of the NWs can be observed, and only very thin and short NWs with a diameter of 24 nm and aspect ratio of 6 were obtained.

By using Al- and Ga-doped seed layers, the growth results are different compared to that one observed for the undoped ZnO seed layers. In the case of Al-doped layers and highest growth temperature of $T = 950^\circ\text{C}$, a well-oriented growth of vertically aligned NWs is observed but only for Al-concentration of $x = 3.5$ at%. These NWs have a diameter of about 80 nm and an aspect ratio of 30. For other doping concentrations, the NW growth is suppressed and only growth of honeycomb-like structures is obtained. These honeycomb-like structures were not observed on the undoped seed layers and are typical for the growth on the doped seed layers. Interestingly, that with reduction of the growth temperature to $T = 700^\circ\text{C}$, NWs were obtained on the seed layer with a concentration of $x = 7$ at% only and the growth on the seed layers with $x \leq 3.5$ at% is suppressed. A further reduction of the growth temperature leads to decrease of the optimum Al concentration which supports the growth of NWs, i.e. at $T = 600^\circ\text{C}$ NWs are obtained for the doping concentration of $x = 2$ and $x = 3.5$ at%, whereas for $T = 400^\circ\text{C}$, the growth is observed on the seed layers with $x = 1$ and 2 at%. Note, all NWs are well-oriented vertically, and for

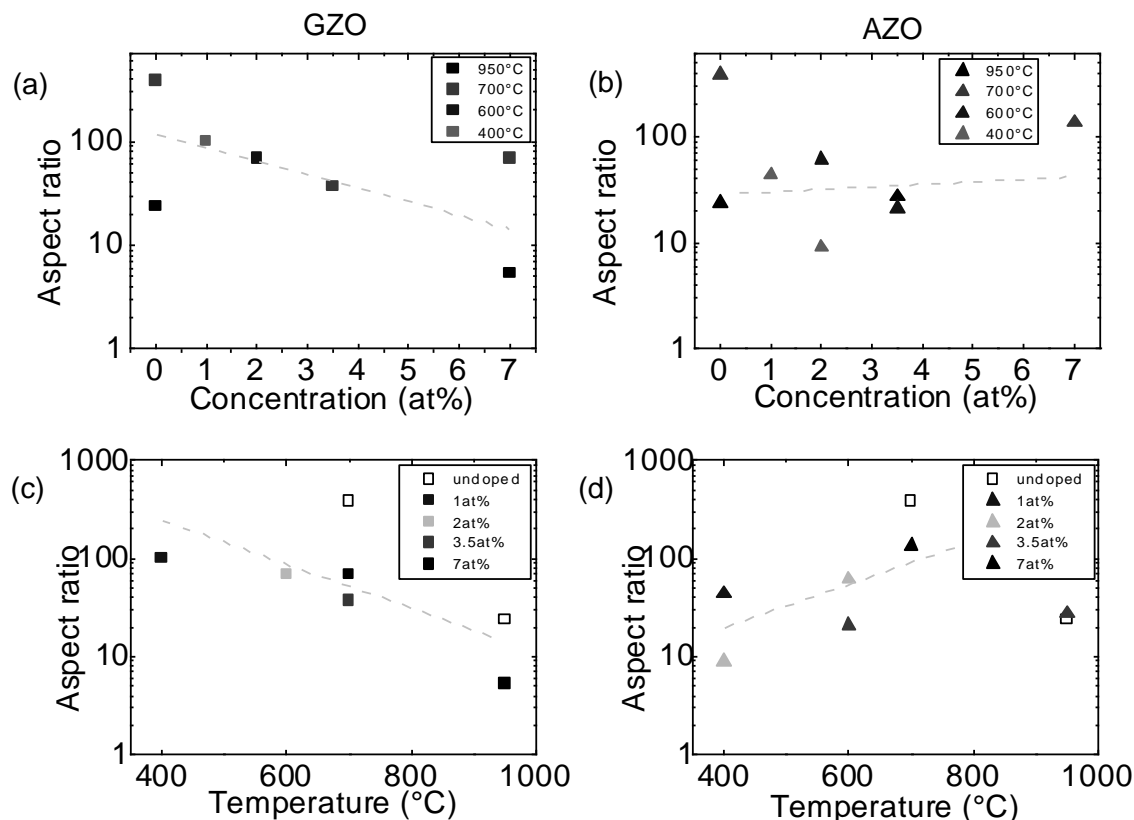


Fig. 4. NW aspect ratio as a function of the doping concentration (a,b) and growth temperature (c,d) for the Ga-doped (a,c) and Al-doped seed layers (b,d).

$T = 400^\circ\text{C}$, NWs are grown as an ultrathin array with a diameter of $d \leq 7$ nm and an aspect ratio of 45. For the concentrations which does not support the growth of NWs at given temperature, the growth of a honeycomb-like structures is observed.

The growth on the Ga-doped seed layers is slightly different at temperature of $T=950^\circ\text{C}$ compared to that one observed on the Al-doped layers. For this growth temperature, there are no NWs are observed on the seed layer doped with $x=3.5\text{at}\%$. However, for the doping concentration of $x = 7\text{at}\%$, growth of elongated pyramid-like structure was obtained. For other concentrations and growth temperatures, the results are mostly similar to those ones grown on the Al-doped seed layers. Growth of ultrathin NWs with a diameter $d \leq 7$ nm and an aspect ratio of about 100 was obtained on the seed layer doped with $x = 1$ at% of Ga and by using growth temperature of $T = 400^\circ\text{C}$.

In the work of Kaebisch et al [17], an impact of the Al dopants in the seed layer on the NW growth process is observed as well. They attributed this behavior to a change of the surface polarity from an O-terminated surface of the undoped ZnO layer to a Zn-terminated one of the Al-doped layers. In their case, on the doped layers, the honeycomb-like structures were fabricated instead of NWs. The observed growth of the honeycomb structure for the Al- and Ga-doped layers in the experiments

presented here, would also indicate such a change of the surface polarity. In order to verify the change, the polarity of the seed layers were determined by using an etching method described in Ref. 24. Accordingly to that method, the seed layers were etched in a diluted HCl acid with a concentration of 1:100 for 30 s and the etching pattern indicates a type of the polarity. Note, that for the mentioned concentration, an etching rate is expected to be of about 1 nm/s. This experiment revealed that only for the undoped seed layer as well as for Al-doped layers with $x = 1$ at%, an O-terminated surface was found which manifested itself by a pyramidal etching pattern. Other seed layers have a crater-like pattern which indicates a Zn-termination. However, in contrast to the conclusions made by Kabisch et al., the change of the polarity of the surface seems to be unlikely for the difference of the observed growth behaviors since the NWs are able to be fabricated even on the Zn-terminated surfaces.

A change of the observed NW growth results can be caused by a variation of the growth mechanism [10,11] via a change of the free energy, which can be given by: $\Delta F = F_m + F_i - F_s$ [25]. Here F_m , F_i , and F_s represent the free energy of the depositing material, the interface, and the surface, respectively. Obviously, the surface roughness and crystal quality described above, have an impact on the surface free energy. However, their impact is not sufficient in order to change the entire growth

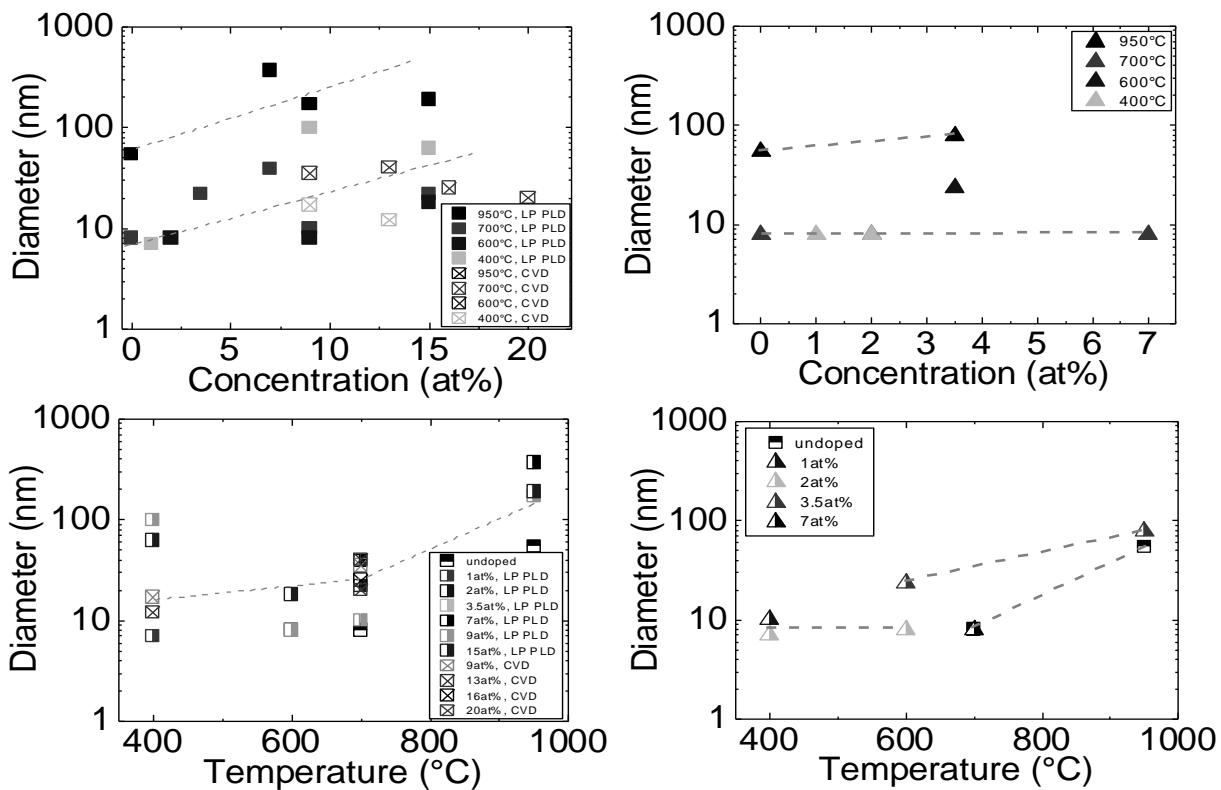


Fig. 5. The diameter of the NWs as a function of the doping concentration (a,b) and growth temperature (c,d) for the Ga-doped (a,c) and Al-doped seed layers (b,d).

mechanism. For example, for the Ga-doped seed layers, the grain size was determined almost the same, whereas for the Al-doped ZnO layers, the grain size increases with increasing Al concentration. However, for both types of the seed layers, the growth results are observed almost the same and fabricated NWs have similar diameter and aspect ratio. This result is in a contradiction to the results obtained by Ting et al. [26] which conclude that the NW diameter increases with the grain size. Moreover, neither an increase of the diameter of the NWs with decreasing of the surface roughness [19] nor another correlations were found. Note that a change of the surface roughness and the grain size caused by the elevated temperature during the growth process can be excluded since XRD and AFM measurements performed on the reference samples and annealed under deposition conditions did not reveal a sufficient change of the seed layer morphology.

Thus, a sum of the free energy of the depositing material (i.e. F_m) and the free energy of the interface of deposited ZnO (F_i) has a strong and significant impact on the change of the growth mechanism. However, the experimental determination of these free energies is technically challenging by using mentioned HP PLD chamber. For the F_m investigation a mass spectrometer should be integrated inside the chamber, whereas for the F_i determination, a theoretical model based on the Monte Carlo simulations is needed [27].

In Fig 4 and 5, aspect ratio and diameter of the grown NWs as a function of the doping concentration of the seed layers and the growth temperature are presented respectively. The aspect ratio of the NWs grown on Ga-doped ZnO layers decreases with increasing doping concentration, whereas it decreases with increasing temperature. At the same time, an increase of the NW diameter with increasing Ga concentration and growth temperature is observed. For the growth on the Al-doped layers, a slightly different situation occurs. Here, the NW aspect ratio has no behavior as a function of the Al doping concentration but increases with the growth temperature.

Thereby, the Ga doping of the ZnO seed layer has a stronger impact on the NW diameter than the doping of the layers with Al. This effect might be explained by the larger size of Ga dopants which are probably more attractive for the deposited ZnO particles, i.e. the particles remain close to the surface of the seed layer and their motion toward the NW axis is suppressed. Thus, the lateral growth rate is enhanced, i.e. the NW diameter increases, whereas the vertical growth is reduced, i.e. the NW length decreases. Also, seems that the kinetic energy of the moving ZnO particles, i.e. particles which were deposited but not yet crystallized, strongly depends on the growth temperature. Low kinetic energy might be

responsible for the lateral mobility and the lateral growth rate of the NWs on the both types of the seed layers.

Conclusions

In order to summarize the work, following conclusions should be made:

- 1) Al and Ga dopants in the ZnO seed layers have a significant impact on the NW growth process. They effect on the surface free energy via surface morphology, crystal quality of the layers and other surface parameters and thus can change the growth mechanism of the NWs.
- 2) The NWs can be fabricated at $T = 400^\circ\text{C}$. This temperature is far below the typical PLD-used temperature, allows to protect metallic contact lines in the CMOS structure and thus, the NWs can be integrated into this technology.
- 3) By using a low-temperature process, a well-oriented vertical array of ultrathin NWs can be obtained on the seed layer doped with $x = 1\text{at\%}$ of Al or Ga. These NWs have a typical diameter $d < 10$ nm, which is comparable with a Bohr radius.

References

1. V. A. Coleman and C. Jagadish, Basic Properties and Applications of ZnO, edited by C. Jagadish and S. Pearton, The Netherlands, Amsterdam, Elsevier Limited, Chapter 1, (2006).
2. A. R. Hutson, Phys. Rev. Lett., 4, 10, 505, (1960).
3. C. P. Dietrich and M. Grundmann, Wide Band Gap Semiconductor Nanowires: Low-Dimensionality Effects and Growth, edited by V. Consonni and G. Feuillet, USA, Hoboken, Wiley-ISTE, Chapter 22, (2014).
4. M. Grundmann, The Physics of Semiconductors, Germany, Heidelberg, Springer-Verlag, 3 edition, (2016).
5. S. Xu, et al., Adv Mater., 22, 4749, (2010).
6. J. Mei, et al., Procedia Eng., 47, 462, (2012).
7. R. Dauksevicius, et al., Procedia Eng., 120, 896, (2015).
8. Z.L. Wang, Mater. Sci. Eng. R, 64, 33, (2009).
9. S. M. Frolov, et al., MRS Bulletin, 38, 809, (2013).
10. J. S. Horwitz and J. A. Sprague, Pulsed Laser Deposition of Thin Films, edited by D. B. Chrisey and G. K. Hubler, USA, New York, 229, Wiley-Interscience, (1994).
11. M. Lorenz, Zinc oxide as transparent electronic material and its application in thin film solar cells, edited by K. Ellmer, A. Klein and B. Rech, Germany-USA, Berlin-Heidelberg-New York, Springer, Chapter 6, (2006).
12. A. Shkurmanov, et al., Nanoscale Res. Lett., 12, 134, (2017).
13. M. Lorenz, et al., Appl. Phys. Lett., 86, 14, 143113, (2005).
14. A. Shkurmanov, et al., Procedia Eng., 168, 1156, (2016).
15. T. Michalsky, et al., Eur. Phys. J. Appl. Phys., 74, 30502, (2016).
16. M. Willander, et al., Nanotechnology, 20, 332001, (2009).
17. S. Kabisch, et al., Appl. Phys. Lett., 23,10, (2013).

18. S. Sedky, et al., IEEE Trans. on Elec. Dev., 48, 2, 377, (2001).
19. H. Ghayour, et al., Vacuum, 86, 101, (2011).
20. A. Patterson, Phys. Rev., 56, 978, (1939).
21. A. P. Samantilleke, et al., Nanoscale Res. Lett., 6, 309, (2011).
22. A. Rahm, et al., Appl. Phys. Lett., 88, 31, (2007).
23. Y. W. Heo, et al., J Nanosc. Nanotech. 14, 12, 9020, (2014).
24. A.N. Mariano and R.E. Hanneman, J. App. Phys., 34, 2, 384, (1963).
25. A.A. Chernov, Modern crystallography III – Crystal Growth, edited by E. Givargizov, Germany, Berlin-Heidelberg, Springer, (1984).
26. J.M. Ting, et al., J. Am. Ceram. Soc. 92, 11, 2718, (2009).
27. A. Shkurmanov, ZnO-based nanostructures by PLD: growth mechanism, doping and geometry, Universität Leipzig, 2017